Spray characterization of the cutting extinguisher

Michael Försth, Raúl Ochoterena, Johan Lindström

SP Technical Research Institute of Sweden

Fire Technology

SP Arbetsrapport 2012:14

Spray characterization of the cutting extinguisher

Michael Försth, Raúl Ochoterena, Johan Lindström

Abstract

Spray characterization of the cutting extinguisher

Experimental measurements using interferometric drop sizing show that the spray from the cutting extinguisher is characterized by small droplets. The following characteristic diameters were measured at 10 m distance from the nozzle using 260 bar injection pressure: arithmetic mean diameter $d_{10}\approx 70$ µm, Sauter mean diameter $d_{32}\approx 170$ µm , and volumetric mean diameter $d_{30}\approx 110$ µm. The latter value confirms previous theoretical estimations that $d_{30}\approx 0.1$ mm. The velocity at this distance from the nozzle was approximately 7 ms^{-1} in the spray core. Droplet diameters decrease significantly when foaming agents are mixed into the water, d_{10} drops to 40 µm and d_{32} to 140 µm. Droplets also seem to be smaller outside the spray core, d_{10} drops to 40 µm and d_{32} to 100 µm at an off center distance of 80 cm from the spray axis. The volumetric capacity was 57 $lmin^{-1}$. These measurements confirm earlier explanations of the efficiency of the cutting extinguisher, and also lead to more detailed understanding of the extinguishing effect.

Key words: spray, water mist, high pressure, cutting extinguisher, droplet size, histogram, laser diagnostics, GSV, ILIDS

SP Sveriges Tekniska Forskningsinstitut
SP Technical Research Institute of Sweden

SP Arbetsrapport 2012:14
ISSN 0284-5172
Borås 2012

Contents

Preface

This work has been funded by a grant from Vinnova within the Forska & Väx program, grant nr. 2012-00499. Cold Cut Systems was the client ordering the project from SP. Cold Cut systems, hereafter referred to as the client, was responsible for choosing, providing and assembling the equipment which were tested in the experimental campaign. The support of Vinnova and Cold Cut Systems is gratefully acknowledged.

Special acknowledgement is given to Torwald Snickars and Patrik Söderberg at Cold Cut Systems who participated in most of the experimental work and who carefully read and commented this report. Torwald Snickars was the photographer of all photos presented in this report.

Summary

This study presents the first experimental measurement of the droplet diameters from the cutting extinguisher. The laser diagnostic technique GSV (Global Sizing Velocimetry) was used to measure drop size distributions and velocities. Comparative measurements were also performed using piercing nozzles and conventional nozzles in order to understand the difference between the different systems. The measurements conducted using these systems were, however, complicated by the existence of large droplets outside the dynamic range of the measurement system.

Experimental measurements show that the spray from the cutting extinguisher is characterized by small droplets. The following characteristic diameters were measured at 10 m distance from the nozzle using 260 bar injection pressure: arithmetic mean diameter $d_{10}\approx 70$ µm, Sauter mean diameter $d_{32}\approx 170$ µm , and volumetric mean diameter $d_{30}\approx 110$ µm. The latter value confirms previous theoretical estimations that $d_{30}\approx 0.1$ mm. The velocity at this distance from the nozzle was approximately 7 ms^{-1} in the spray core. Droplet diameters were found to decrease significantly when foaming agents are mixed into the water, d_{10} drops to 40 µm and d_{32} to 140 µm. Droplets also seem to be smaller outside the spray core, d_{10} drops to 40 µm and d_{32} to 100 µm at an off center distance of 80 cm from the spray axis. The volumetric capacity was 57 $lmin^{-1}$.

These measurements confirm earlier explanations of the efficiency of the cutting extinguisher, and also lead to a more detailed understanding of the extinguishing effect. Cooling, inerting and radiation absorption becomes more effective with these small droplet diameters compared to systems with larger droplets. Furthermore, the fact that small droplets are more prone to follow the air flow than to fall to the floor means that the time available for these suppression mechanisms to act on the fire becomes longer with smaller diameters. The high pressure, resulting in a high speed and high flow, creates a high momentum spray that pushes the water mist long distances into an enclosure fire, making it possible to act on fires distant from the nozzle exit despite the small droplet size.

1 Introduction

Several studies have shown that high pressure water mist systems are efficient in fire suppression [1, 2] . In addition to efficient fire suppression this technology also leads to a reduced quantity of wastewater and less property damage due to water.

The focus of these previous studies has to a large degree been on tactics [3] and it has for example been shown that the efficiency is improved when the jet is directed onto hot surfaces and hot fire effluents. The explanation for this is that high temperatures enhance vaporization and that water vapor, as compared to liquid phase water, leads to decreased oxygen concentrations close to the fire due to dilution, which inhibits the combustion process.

However, the size and velocity distributions of the droplets in these sprays has only been theoretically estimated and detailed measurements have been lacking. This information is required in order to fully understand and develop high pressure water mist systems. In this project detailed measurements of droplet size and velocity distributions of the cutting extinguisher [4] were performed. Comparative measurements of some non-high-pressure systems were also performed.

2 Brief spray theory

In this section some important aspects of the physics of sprays are briefly described [5].

2.1 Atomization of an ejected liquid

Atomization is the process by which a homogeneous liquid, injected into for example ambient air, breaks up into ligaments and droplets due to disruptive internal and external forces. If no disruptive forces exist the surface tension will pull the liquid into a sphere [6]. In reality however there are internal forces, such as turbulence for example, and external forces, such as air pressure, which will distort the liquid and/or split the droplets into several smaller more or less spherically shaped droplets.

Atomization can be divided into two phases: primary and secondary atomization. Primary atomization is caused mainly by purely internal forces in the liquid. Secondary atomization is caused by aerodynamic forces, caused by the droplets travelling through the ambient air, overcoming the restoring forces of the droplets [7], which mainly are surface tension and viscous forces.

The dynamic pressure on a droplet surface exposed to a perpendicular air flow with speed v is given by:

$$p_{dyn} = \frac{1}{2}\rho_{air}v^2 \tag{1}$$

The force that the dynamic pressure exhibits on, for example, a droplet is proportional to the dynamic pressure multiplied by the cross-sectional area of the droplet. Since the droplet does not expose an infinite perpendicular area towards the air flow there is a proportionality constant C_{drag}, the drag coefficient. The drag force on a droplet becomes:

$$F_{drag} = \frac{\pi C_{drag}}{8} \rho_{air} v^2 d^2 \tag{2}$$

The velocity v is the relative velocity between the droplet and the air. In this theoretical model the liquid is assumed to be ejected into quiescent air and v is therefore the droplet velocity. The drag force F_{drag} acts as a deforming force. The surface tension on the other hand acts as a restoring force. The contracting force around the perimeter of a droplet, F_σ, is given by the surface tension σ multiplied by the length of the circumference:

$$F_\sigma = \pi \sigma d \tag{3}$$

The ratio F_{drag}/F_σ is:

$$\frac{F_{drag}}{F_\sigma} = \frac{C_d}{8} \frac{\rho_{air} v^2 d}{\sigma} = \frac{C_d}{8} We \tag{4}$$

Where We is the dimensionless Weber number:

$$We = \frac{\rho_{air} v^2 d}{\sigma} \tag{5}$$

The Weber number is the ratio between the fragmenting aerodynamic force, due to the dynamic pressure, and the cohesive force due to surface tension [8]. A droplet subjected to a relative air velocity can be assumed to be unstable, i.e. prone to breakup, when the deforming drag force is equal to or greater than the restoring surface tension, that is when expression (4) is equal to or greater than unity. The theoretically maximum stable droplet size, d_{max}, can then be calculated from:

$$d_{max} = \frac{8\sigma}{\rho_{air} v^2 C_{drag}} \tag{6}$$

This is often expressed in terms of the critical Weber number

$$We_{crit} = \frac{8}{C_{drag}} \tag{7}$$

Critical Weber numbers have been found to be in the range 15-32 by Korsunov and Tishin [9] for transformer oil and in the range 12-22 by Johnson and Woodward [10] for heat transfer fluids. Kolev [11] reported critical Weber number between 5-20 for low viscosity liquids with 12 being the most common value. A list of results from studies on We_{crit} for different liquids and operating conditions can be found in reference [12].

Here, it is interesting to preempt the experimental results in Section 4.2 and check what the typical theoretical maximum droplet diameter is, according to critical Weber number theory, for the cutting extinguisher used in this study. The surface tension σ of water is 73 mNm^{-1}. The density of air is 1.2 kgm^{-3}. Assuming an initial velocity of 220 ms^{-1} and a critical Weber number of 20 gives :

$$d_{max} = \frac{We_{crit}\sigma}{\rho_{air}v^2} \approx \frac{20 \cdot 73 \cdot 10^{-3}}{1.2 \cdot 220^2} \approx 25\ \mu m \qquad \textbf{(8)}$$

Many droplets with larger diameters are found in the experiments. One should remember that expression (8) assumes that the relative speed of the droplet as compared to the air is the same as the relative speed of the droplet as compared to the atomizer. This is not the case since the high flow of droplets will induce an airflow in the same direction as the spray. This is pointed out in reference [13] where it is also noted that when We_{crit} is reached the droplets start to break up. If the droplet is decelerated the breakup process might stop. On the other hand the aerodynamic drag might distort the droplet in such a way that the break up should be promoted. In short d_{max} in expression (8) is not more than a qualitative estimation of the maximum droplet diameter, indicative but not absolute.

2.2 Droplet size distributions

Small droplets (< 2 mm) are in general close to spherical in shape and can therefore be described using a single parameter [14]. Larger droplets are typically distorted by gravity. Different parameters are then used depending on the application. The parameters used in this report is presented below. Sometimes the median diameter is used to characterize a spray. This parameter is of lesser interest for water mist, however, since large droplets will carry significant amounts of water and conversely the amount of water in the smaller droplets is low. Since very large droplets are not at all reflected in the median diameter this parameter has not been considered further in this study.

2.2.1.1 Length Mean Diameter (arithmetic mean diameter)

$$d_{10} = \frac{\int_0^\infty d f_d \, dd}{\int_0^\infty f_d \, dd} \qquad \textbf{(9)}$$

where f_d is the distribution of droplets in a spray.

2.2.1.2 Sauter Mean Diameter, SMD

$$d_{32} = \frac{\int_0^\infty d^3 f_d dd}{\int_0^\infty d^2 f_d dd} \tag{10}$$

where d_{32} is the diameter of a droplet whose volume to surface ratio is the same as the volume to surface ratio of the entire spray. d_{32} is particularly important when mass transfer and the active area per volume is important [6, 8]. Therefore d_{32} is an appropriate parameter for water mist since the purpose with the small droplets in water mist is to achieve large surface related effects, such as cooling and evaporation, while using small volumes of water.

2.3 Thermodynamic boundaries of water sprays

2.3.1 Heating and vaporization of water

The energy necessary to heat the water from the injection temperature T_0 to the boiling point T_{boil} (373 K at atmospheric pressure), for a water volume V, is;

$$W'''_{heat} = \frac{W_{heat}}{V} = c_p \rho (T_{boil} - T_0) \tag{11}$$

where

c_p is the specific heat capacity of water at constant pressure, c_p =4.18·10^3 Jkg^{-1}K^{-1}[15]. c_p is essentially independent of temperature in the relevant temperature range 293-373 K.

ρ is the density of water, ρ = 9.98·10^2 kgm^{-3} at 293 K [15]. ρ decreseas by 4% when the temperature is increased to 393 K but this has no effect on the calculation above since the injected volume V increases accordingly.

When the water has reached T_{boil}, all energy absorbed contributes to the evaporation phase transition from liquid to vapor (gas). The energy required to evaporate a volume V at T_{boil} is given by

$$W'''_{vap} = \frac{W_{vap}}{V} = \Delta H_{vap} \rho \tag{12}$$

where

ΔH_{vap} is the heat of vaporization of water at constant pressure, ΔH_{vap} = 2.26·10^6 Jkg^{-1} [15].

Assuming the injection temperature T_0 is 293 K we obtain the ratio

$$\frac{W'''_{heat}}{W'''_{vap}} = \frac{c_p(T_{boil} - T_0)}{\Delta H_{vap}} = 0.15 \quad \textbf{(13)}$$

This means that the 87% of the heat absorbed from the fire goes to vaporization and 13 % goes to heating of the liquid water.

The discussion above has assumed that the water is in its bulk form. For droplet sizes considered in this report, the specific heat capacity and the heat of vaporization do not deviate significantly from the bulk value, but this is not necessarily true for very small droplets (<0.01 μm).

The heating and vaporization of the water cools the fire gases. The cooling rate, however, depends on the rate of heat transfer into the droplets. The interface for this process is the surface of the droplet and the droplet area per droplet volume is therefore a determining parameter for estimating the rate of cooling of the fire gases, see below.

Finally the specific heat capacity at room temperature and constant pressure is 2.0 $kJkg^{-1}K^{-1}$for water vapor and 1.0 $kJkg^{-1}K^{-1}$ for air. Water vapor is in other words relatively efficient, as compared to air, in cooling the gases after the evaporation.

2.3.2 Atomization

When a liquid of volume V is atomized into a monodispersed spray of N droplets each droplet takes a volume given by

$$\frac{V}{N} = \frac{4}{3}\pi r^3 \quad \textbf{(14)}$$

where r is the radius of the droplets.

For a spray atomized into N monosized droplets the total area is

$$A = Na = \left(\frac{3V}{4\pi r^3}\right)(4\pi r^2) = \frac{3V}{r} \quad \textbf{(15)}$$

Figure 1 shows expression (15) in graphical form.

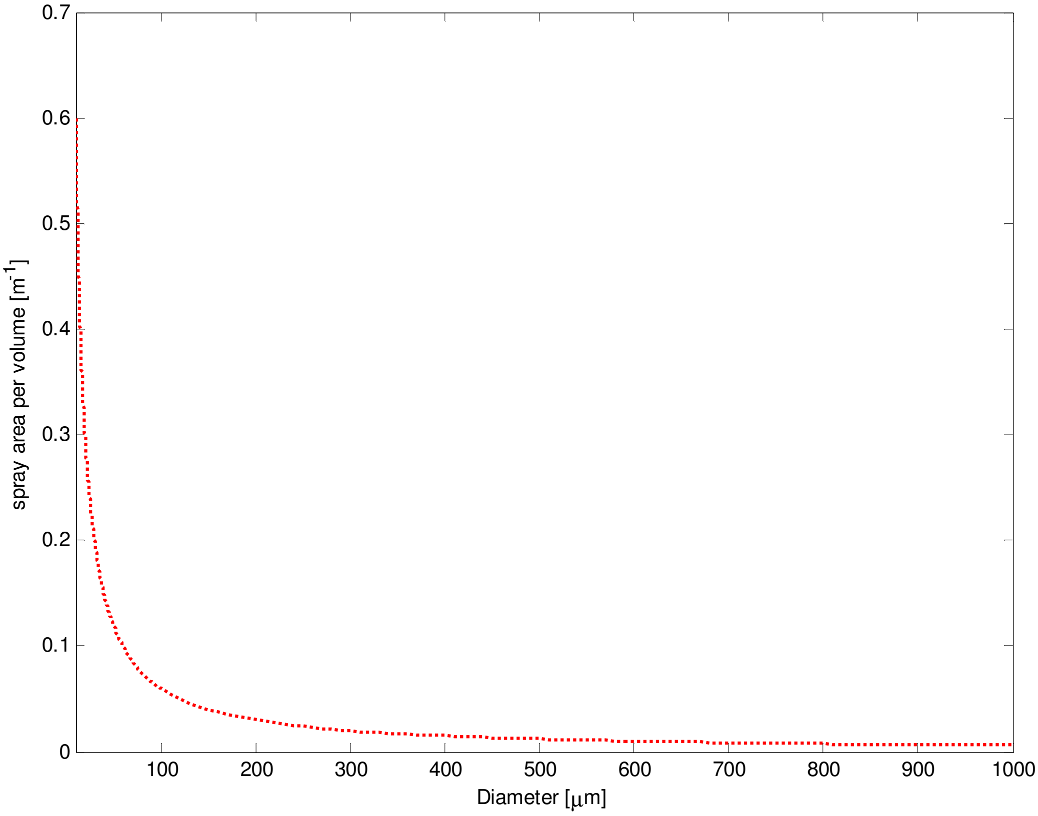

Figure 1 Spray area per volume as a function of droplet diameter. This applies for a single droplet of for a monodispersed spray.

3 Material and Methods

3.1 The investigated fire extinguishing systems

In this test series different fire extinguishing systems were tested. All materials were supplied to SP by the client. Also, the client determined the operating conditions (flow, pressure and location of the measuring volume) for every test. The reason for investigating different systems was to compare and assess the differences in droplet size distribution between these systems, to study how different systems behave when extinguishing a fire.

The different systems used in the study were chosen as they are representative of tactical systems deployed commonly in Sweden. The systems chosen for comparison were piercing nozzles (attack fog spear and diffuser fog spear) and fog nozzles (adjustable wide angles fog nozzles). The systems are all described in more detail below.

Note that when using the piercing nozzles and fog nozzles described below, the pump had a pump pressure of 40 bar and was equipped with a ¾″ hose, 80 m long. Even though the hose was completely uncoiled the pressure drop was very large, meaning that we could only achieve max 21 bar pressure at the nozzle exit with the piercing nozzle instead of the intended 30 bar.

3.1.1 Cutting extinguisher coldcut™ cobra modell C360B

The coldcut™ cobra fire extinguishing technique can be divided into two different parts. In similarity to other high pressure water mist systems the cobra extinguishes fires using the benefits from water mist. The main difference to other high pressure water mist systems is that the cobra can cut through building materials using an abrasive additive and water. By combining these two parts the cobra method offers the potential for safe attack on an interior fire using gas cooling from an outside position. The nozzle diameter that was used in the tests at SP was 2.3 mm. This nozzle will be referred to as “Cobra” in the next chapter.

Figure 2 The cutting extinguisher “cobra”.

3.1.2 Piercing nozzles

Piercing nozzles or fog spears [16] are mainly used in Sweden in situations where it is difficult to access the fire. Different examples for this are when the fire is situated in walls, roofs, attics and double floors. Fog spears are also commonly used as demarcation lines and to cool fire gases before attack and ventilation. Fog spears can be used for both a conventional pressure system (~10 bar) and for enhanced low pressure systems (~40 bar). When using a fog spear through a wall the firefighter either needs to have an existing hole into the building to put it in or make one with for example a drill. In roof application the spear might be hammered through the construction.

3.1.2.1 Attack fog spear

There are different types of fog spears depending on the fire, the mode of attack and the building. The nozzle pressure can be about 30 bar and have a water flow of 80 l/min when using a fog spear attached to a pump with enhanced pressure (40 bar at pump). This type of fog spear is used for active suppression of the fire. The attack fog spear used for comparison in this study is shown in action in Figure 3. This nozzle will be referred to as the "attack fog spear" in the next chapter.

Figure 3 The attack fog spear.

3.1.2.2 Diffuser fog spear

Another type of typical fog spear has a diffused water. Otherwise, it has the same pressure and water flow characteristics as the attack fog spear described above. This type of spear is mainly used to restrict further spread of the fire. The diffuser fog spear used in this study is shown in action in Figure 4. This nozzle will be referred to as the "diffuser fog spear" in the next chapter.

Figure 4 The diffuser fog spear.

3.1.3 Fog nozzles

The most common method in Sweden has been to use a low pressure systems with 7-10 bar with a water flow that goes up to about 500 l/min. Today the traditional approach has changed slightly and the use of enhanced low pressure systems with a pump pressure of about 40 bar is quite common. In the test series presented in this report, two different adjustable wide angle fog nozzles have been evaluated. Figure 5 shows a fog nozzle in action.

Figure 5 Adjustible wide angle nozzle according to 3.1.3.2.

3.1.3.1 Adjustable wide angle fog nozzle, "Fog nozzle 1"

This nozzle has a ¾″ inlet clutch and is one of the most commonly used nozzles in Sweden. The nozzle is designed to be used with enhanced low pressure pumps, that is 40 bar at pump, as well as with conventional pumps, that is 10 bar at pump. The nozzle was evaluated by Lund's Technical University together with Greater Stockholm's fire brigade, using 10 bar pump pressure, and was found to be the best nozzle among those who were commonly used in Sweden at that time [17]. This nozzle will be referred to as the "Fog nozzle 2" in the next chapter.

3.1.3.2 Adjustable wide angle fog nozzle, “Fog nozzle 2”

This fog nozzle is relatively new on the market and has some features compared to fog nozzle in Section 3.1.3.1. The largest difference in how this nozzle perform compared to the other enhanced low pressure nozzle in this study is that it gives water mist droplets directly when you open the valve, even when it is only slightly open [18]. Also this nozzle is designed to be used with enhanced low pressure pumps, that is 40 bar at pump. This nozzle will be referred to as the “Fog nozzle 2” in the next chapter.

3.2 Laser diagnostics for spray characterization

In order to correctly assess droplets and velocities in a spray it is necessary with a non-intrusive in situ measurement method. Due to the liquid phase of the droplets it would, for example, not be possible to collect them and thereafter characterize their diameters. Laser diagnostics offer the required properties and have therefore been selected as the measurement method of choice in this project. In this section the Global Sizing Velocimetry (GSV) method, used in this project, is briefly described.

3.2.1 Particle Imaging Velocimetry (PIV)

Particle Imaging Velocimetry [19] is a method to determine two-dimensional flow field velocities in a plane. A more advanced form of the method, stereo-PIV, can be used to derive the third velocity component.

A cross-section of the spray is illuminated using laser light formed into a thin sheet. The scattered light is detected using a camera. The illumination is conducted using two laser pulses with a short time separation where images are recorded for each laser pulse. The resulting two images are compared and the distance and direction the imaged objects have moved during the time separation reflects the velocity field. Normally the air is seeded with small particles to provide reference objects whose motion can be imaged, but when measurements are made on a spray the droplets of the spray can be used directly.

3.2.2 Interferometric Laser Imaging for Droplet Sizing (ILIDS)

Interferomteric Laser Imaging for Droplet Sizing [20, 21] measures the size of the droplets in the measuring volume based on its interference pattern after being impinged on by a laser pulse. Therefore this method requires that the sprayed liquid can be considered as optically transparent. These measurements cannot be done for optically opaque droplets. This technique can be used to analyze droplets with diameters in the range between 10 to 700 μm.

3.2.3 Global Sizing Velocimetry (GSV)

A simplified description of GSV [22] is that it combines two measurements methods: PIV and ILIDS. In GSV, the ILIDS technique is used but two images are captured of the interference field, with a time delay between the exposures. The spatial position of the droplets in each image is determined. These locations are near the centre of each individual interference pattern. When the droplet locations are known in each image, and the time delay between the images is known, the velocities can be calculated with computerized algorithms similar to those used in PIV.

The diameter limit for GSV is set by the ability of the software to detect and characterize the interference patterns in the images. Below the expression defining these limits are given [23], as well as the numerical values corresponding to the experimental setup used in this project.

$$d_{min} = \lambda X \cdot \left(1 + \frac{1}{M}\right) \cdot f\# \cdot A = 532 \cdot 10^{-9} \cdot 1.13 \cdot \left(1 + \frac{1}{1.2}\right) \cdot 4.0 \cdot 1.5 = 7\mu m \quad \textbf{(16)}$$

where

λ	wavelength
X	constant depending on scattering angle and refractive index
M	magnification of imaging optics
f#	f-number of the camera lens
A	minimum number of oscillations

and

$$d_{max} = \frac{\lambda X \cdot \Delta z}{M\delta B} = \frac{532 \cdot 10^{-9} \cdot 1.13 \cdot 38 \cdot 10^{-3}}{1.2 \cdot 9 \cdot 10^{-6} \cdot 3} \approx 700\ \mu m \quad \textbf{(17)}$$

where

Δz	defocusing of the camera
δ	pixel size
B	minimum oscillation spacing in pixels.

Figure 6 shows a schematic overview of the experimental setup for drop sizing using GSV.

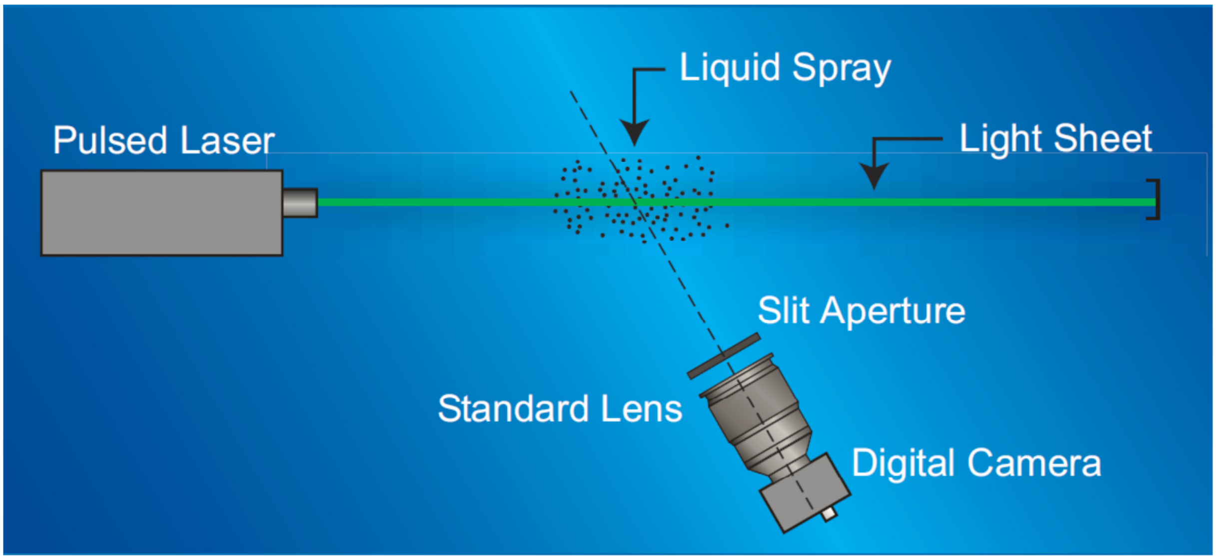

Figure 6 Schematic of the laser diagnostic setup [24].

3.3 Experimental Setup

The cutting extinguisher as well as the other systems investigated were fixed on a mount on a table, 1.2 m above the floor,see Figure 2. The GSV measurement equipment was fixed in a metallic cage as shown in Figure 8 (the cage was also clad with a tarpaulin and the sprays were sectioned through a slit, not shown here). The distance, *z*, between the measurement point and the investigated system was varied by moving the rolling table, see left part in Figure 7. All measurements except two were performed in the center of the spray from the cutting extinguisher, or in the centre of one of the spray plumes from the other systems.

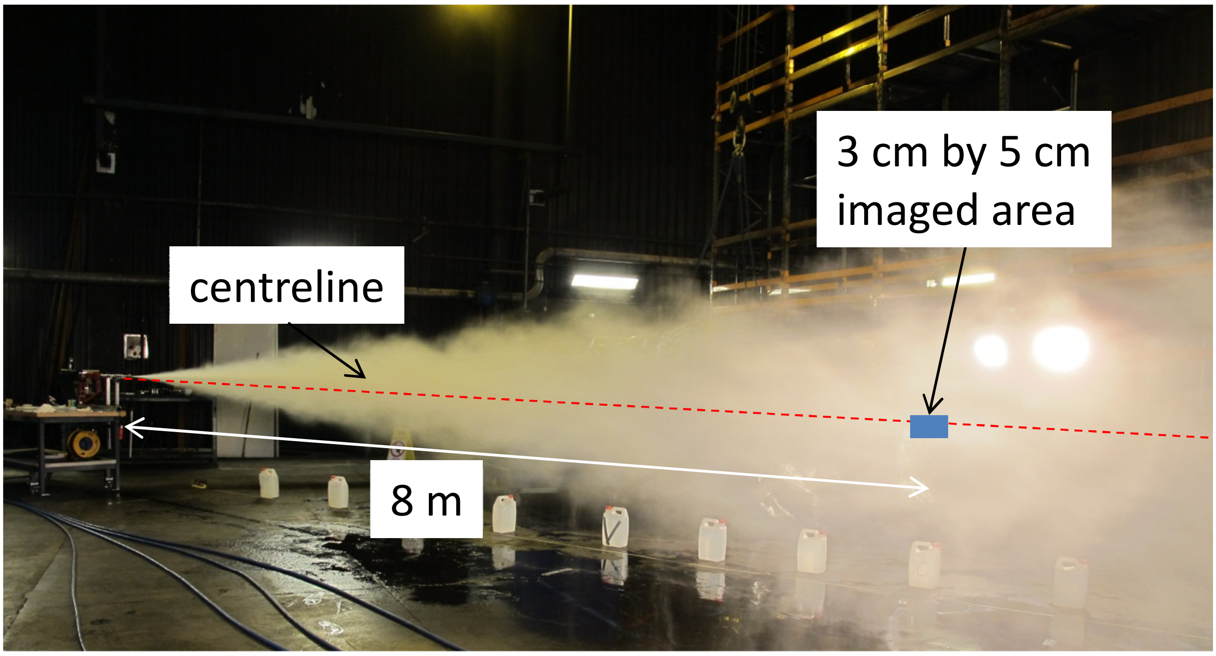

Figure 7 The cutting extinguisher positioned 15 m away from the measurement point. The measurements were performed in a cage (not seen here) to the right of the image. The position of the 8 m measurement is indicated. Note that the measurement cage was not moved, instead it was the table the was rolled to the right in the image when the distance was decreased.

The measurement area is relatively small, on the order of 3 cm by 5 cm. At the same time the angular water distribution was relatively uneven for the fog spears and the nozzles, see Figure 3 to Figure 5. It is possible that size distributions and in particular velocities vary depending on in which part of the spray the measurements are made. The approach in this project was to measure in the most dense parts of the spray. The rationale for this was that most water is transported in the denser parts and therefore the results from those parts are more representative for the fate of the water than the results from less dense parts.

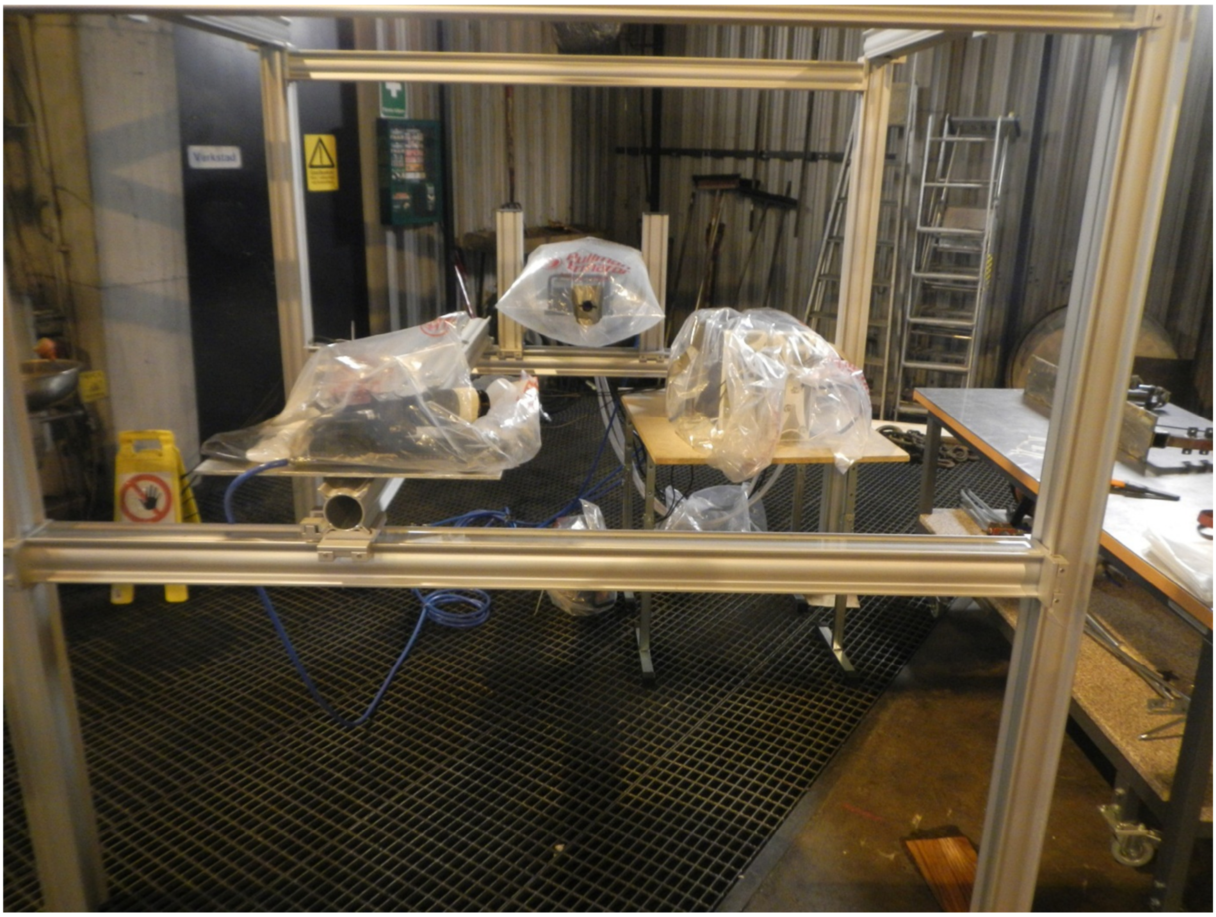

Figure 8 Water proof implementation of the laser diagnostic drop sizing. The aluminium cage was also covered by a tarpaulin, not shown here.

3.3.1 Boundary layer

When a fluid in a free flow enters into contact with a surface, its velocity profile in the region closest to the surface is altered. The velocity of the fluid in contact with the surface experiences a velocity gradient where the fluid molecules closest to the bounding surface have a relative velocity equal to zero and the molecules flowing far away from the bounding surface have the same velocity as the undisturbed flow. The layer where this velocity profile is observed is called the boundary layer, and is it the layer of fluid in the immediate vicinity of the boundary layer where the effects of viscosity are not negligible. If the distance to the boundary layer is long enough, the effects of the boundary layer are unnoticed.

During the experiments to measure the size distributions of the droplets produced by different systems in this project, the spray was sectioned in order to reduce the optical density of the measuring volume. The spray was sectioned using a pair of metal plates with a plane section perpendicular to the axial penetration of the jet. However, the separation between these sectioning plates was designed to be long enough so as to not to perturb the properties of the flow in the measuring volume, i.e. its properties will be similar to that of the undisturbed flow. Figure 9 illustrates the effect of a boundary layer in the flow closest to the surfaces.

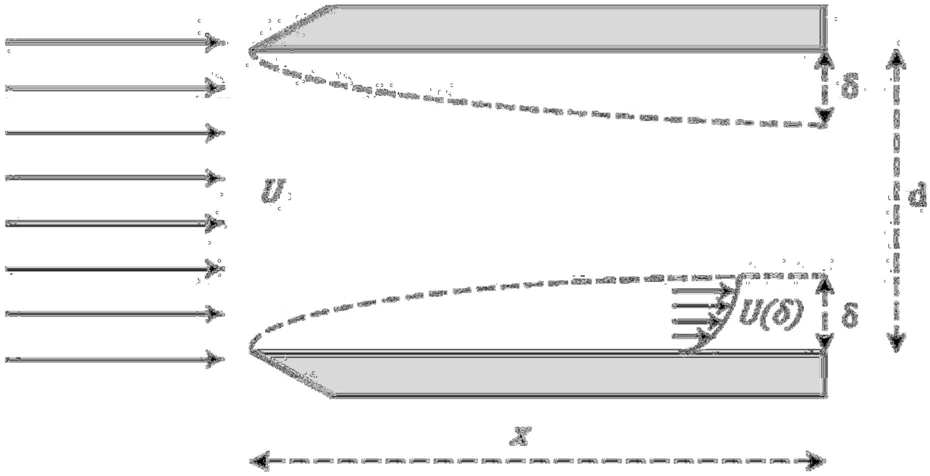

Figure 9. Illustration of the boundary layers created by the two flat metal plates.

The thickness of the boundary layer at the measuring point was calculated according to the boundary layer theory [25] for turbulent flows:

$$\frac{\delta}{x} = \frac{0.16}{\left(\frac{Ux}{\nu}\right)^{\frac{1}{7}}} \qquad \textbf{(18)}$$

where

δ	is the boundary layer
x	length of sectioning hole
U	velocity of undisturbed flow
ν	viscosity of air, $\nu \approx 1.5 \cdot 10^{-5}$ $kgs^{-1}m^{-1}$[25].

The thickness of the boundary layer of a fluid which is mainly composed of air after gliding through a plate with a length x=0.1 m, and which has a free velocity U=5 ms^{-1}, is δ ~ 4 mm. This means that if the plates are separated by a distance larger than 2δ, the flow at the measuring volume just in the middle of the plates can be considered to have the same velocity as the flow upstream the measuring volume. The distance between sectioning plates was much larger than 8 mm and x < 0.1 m; furthermore, the thickness of the measuring volume is smaller than a millimetre. This shows that the sectioning of the spray was non-intrusive.

4 Results

In this section the results for volumetric flow, diameters and velocities are presented. An observation made in particular for the cutting extinguisher is that a few meters from the nozzle exit the spray becomes unstable with vortices developing at the spray edges. This can be observed in Figure 10 and Figure 11 and was also noted visually, and using the hand, at the measurement volume. Further, in the measurement images this can be seen since some images contain densely spaced droplets while other images, for the same operating conditions, contain much more sparsely spaced droplets. It is therefore important to average results over several images. In this study 30 images were analysed for each operating condition, corresponding to a time average of 30 s.

Figure 10. Spray from the cutting extinguisher.

Figure 11. Spray from the cutting extinguisher.

4.1 Volumetric capacity

The volumetric capacity was simply measured by filling a certain volume and measuring the time elapsed.

Table 1 Volumetric capacity for the different systems and pressures.

System	p_{nozzle} [bar]	$\dot{V}$ [$lmin^{-1}$]
Cobra	200	49
	260	57
Attack fog spear	7	55
	21	95
Diffuser fog spear	7	55
	21	90
Fog nozzle 1	6	150
	8	500 [a]
Fog nozzle 2	5	140

a) For this measurement a high capacity low pressure pump (10 bar) was used. For the other measurements (except for the cutting extinguisher) a pump for enhanced low pressure (40 bar) was used.

4.2 Droplet sizes

Figure 12 and Figure 13 show how the droplet size histogram depends on the injection pressure. Since the variation was quite small, from 200 bar to 260 bar, the effect is not very large. It can, however, be observed that when the injection pressure increases the kurtosis of larger droplets is reduced and the histogram becomes more compressed towards smaller droplets, resulting in smaller arithmetic and Sauter mean diameters, d_{10} and d_{32} respectively. The y-axis in the figures shows the number of counts for each size bin. The number of counts is a qualitative indicator of the drop density, but is not necessarily directly proportional to this density.

In two measurements, the foaming agents A-foam and X-fog were mixed in the water (1-2%).

It two measurements the measurements were performed at a radial (horizontally) position of 40 cm and 80 cm, respectively, from the centerline of the spray.

Of the investigated systems it is only the sprays from the cutting extinguisher that consist solely of droplets with diameters below the upper detection limit. This means that these results are reliable and the estimated uncertainty is ±10 %.

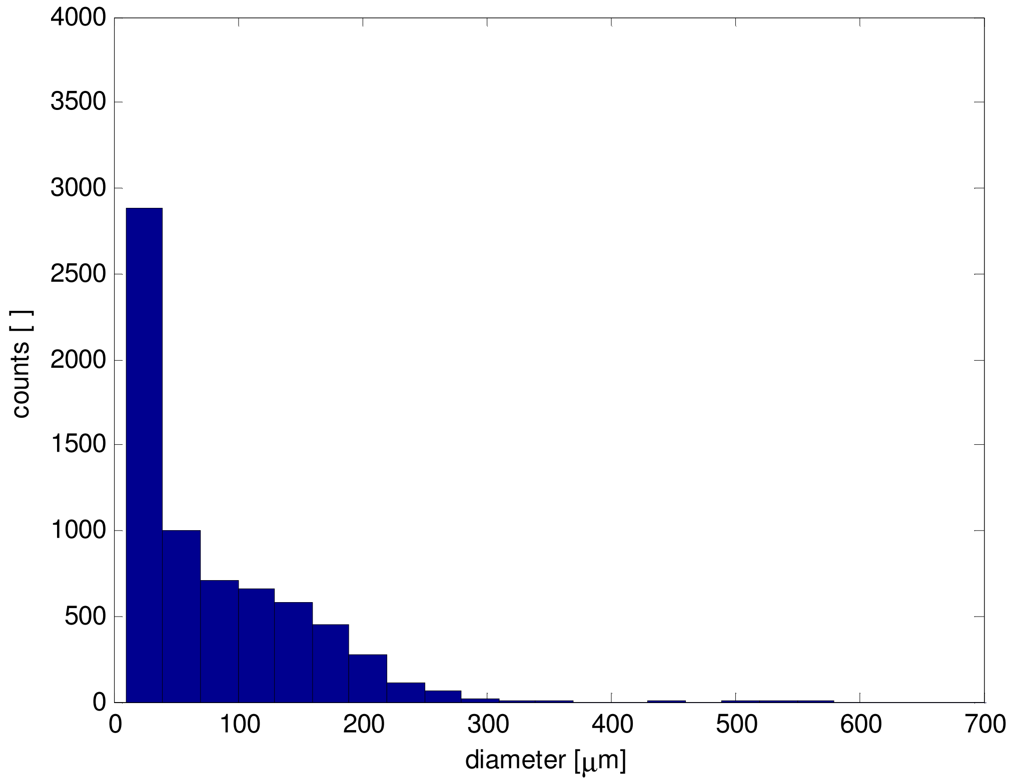

Figure 12 Drop size distribution from the Cobra along the centreline 10 m from the nozzle. p_{nozzle}=200 bar.

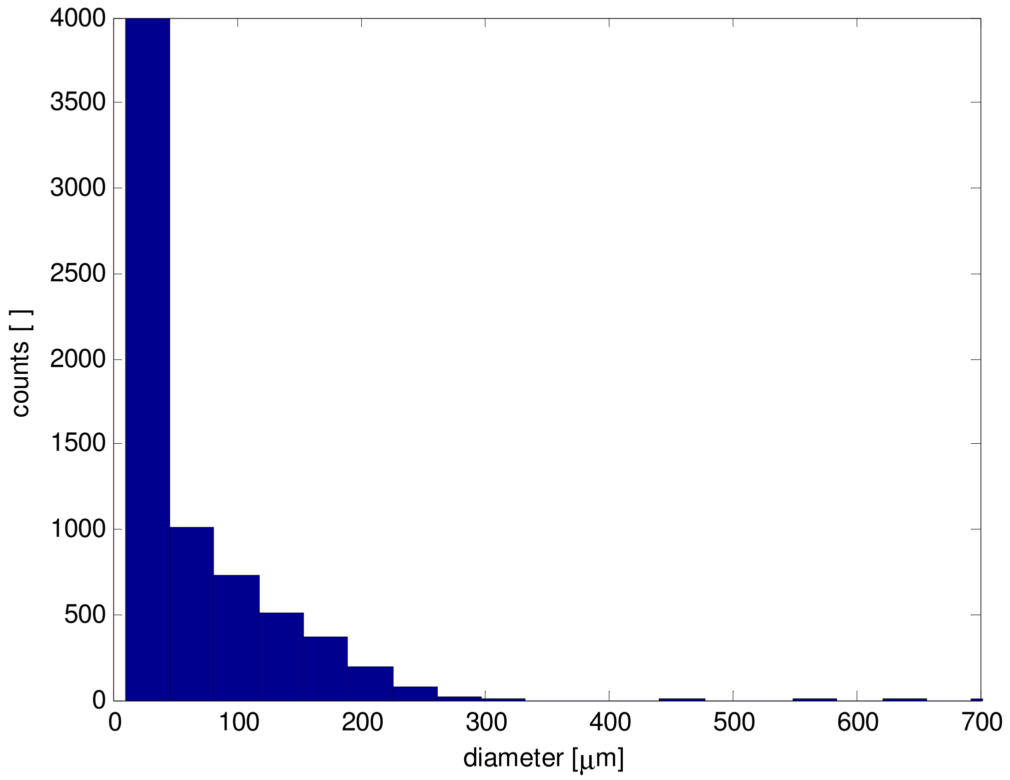

Figure 13 Drop size distribution from the Cobra along the centreline 10 m from the nozzle. p_{nozzle}=260 bar.

For the other systems several droplets with diameters above the detection limit, 700 µm, where visually observed in the images, see for example Figure 14. These droplets could not be sized by the analysis software and are therefore not included in the statistics. This was corrected for in a very rough way in this report. For each configuration (system, pressure, distance) the number of such large droplets were manually visually counted in all 30 interferometry images. These large droplets were assumed to have a diameter of 1000 µm. With these droplets included in the data set the statistical analysis for d_{10} and d_{32} were then performed. The uncertainty for these measures is large for d_{10} and very large for d_{32}.

Figure 14 Visual observations show that a large number of droplets are relatively large in the spray from a nozzle.

The measured or estimated values for d_{10} and d_{32} are shown in Table 2 and Table 3.

Table 2 Arithmethic mean diameter, d10. Values in orange indicates a high uncertainty since droplets above the analysis limit were counted manually.

System	p_{nozzle} [bar]	z [m] / comment	2	4	8	10	15
			d_{10} [µm]				
Cobra	200				60	77	85
	260				46	62	86
	260	A-foam				33	
	260	X-fog				38	
	260	R=40 cm				64	
	260	R=80 cm				43	
Attack fog spear	7			190			
	21			160			
Diffuser fog spear	7		100				
	21		90				
Fog nozzle 1	6 [a]		300[a]				
	8			140			
Fog nozzle 2	5		150				

a) Only 189 droplets detected in total which leads to poor statistics.

Table 3 Sauter mean diameter, d_{32}. Values in red indicates a very high uncertainty since droplets above the analysis limit were counted manually.

System	p_{nozzle} [bar]	z [m] / comment	2	4	8	10	15
			d_{32} [µm]				
Cobra	200				157	174	174
	260				160	170	196
	260	A-foam				149	
	260	X-fog				109	
	260	R=40 cm				127	
	260	R=80 cm				97	
Attack fog spear	7			1000			
	21			900			
Diffuser fog spear	7		800				
	21		700				
Fog nozzle 1	6 [a]		900 [a]				
	8			900			
Fog nozzle 2	5		900				

a) Only 189 droplets detected in total which leads to poor statistics.

4.3 Velocities

The measured horizontal velocities are shown in Table 4.

Table 4 Horizontal velocity

System	p_{nozzle} [bar]	z [m] / comment	2	4	8	10	15
			U [ms^{-1}]				
Cobra	200				[b]	6	4
	260				[b]	7	5
	260	A-foam				6	
	260	X-fog				5	
	260	R=40 cm				4	
	260	R=80 cm				3	
Focused fog spear	7			<1			
	21			1			
Restricting fog spear	7		<1				
	21		1				
Fog nozzle 1	6 [a]		1 [a]				
	8			1			
Fog nozzle 2	5		1				

a) Only 189 droplets detected in total which leads to poor statistics.

b) Due to excessive density of droplets in the images it was difficult for the software to track the individual particles and the results therefore become unreliable, and are not presented here. PIV is recommended for velocity measurements in such dense sprays.

5 Discussion

In this section a general discussion about the measurement results is given followed by a discussion of how the results relate to various mechanisms which are important for water mists in fire extinguishing. The discussion focuses on the areas where small droplets are an advantage. Applications where water mist is typically not used, such as total flooding for example, are not considered in this context.

The results for the cutting extinguisher are in general quite consistent and the spray can be characterized by a d_{10} of 70 µm and a d_{32} of 170 µm.

This more or less confirms previously made assumptions that the volume mean diameter, d_{30}, is approximately 0.1 mm [3, 26]. In fact, calculating d_{30} based on the histogram in Figure 13 gives d_{30} = 107 µm. The volume mean diameter d_{30} is not tabulated in this report since it is of limited value when describing the mechanisms important for water mist [6].

Moreover, measurements with foaming agent show that the diameter decreases significantly, as expected due to the reduced surface tension, resulting in an increased Weber number for a given diameter, see also Section 2.1.

Lastly, off centre measurements indicate that droplet diameters decrease with increasing radius. Since non negligible amounts of the total water flow is transported several decimetres from the centreline this means that the average diameters, averaged over the entire spray cross section, would be expected to be significantly lower than the indicated values, which were measured in the core.

Comparing the droplet sizes for the high pressure water mist system (that is the cutting extinguisher) with conventional systems it is clear that the arithmetic mean diameter d_{10} and the Sauter mean diameter d_{32} are significantly smaller for the cutting extinguisher as compared to the other systems employed in this study. The results for the other systems cannot be used for a quantitative analysis, however, since many droplets were detected with diameters that were too large to be determined by the measurement system. In order to take these into account to a certain degree in the comparison these were compensated for in a fairly coarse way by estimating the proportion of large droplets from experimental pictures. Despite this, it can be concluded that, a large part of the delivered water from these systems was carried in large droplets. Given the large uncertainties for the other systems we will, for the remainder of this discussion, simply assume for conventional systems that d_{10}=150 µm and d_{32}=900 µm. This can be compared with previous studies on for example a residential sprinkler [27] where $d_{10}\approx$200µm and $d_{32}\approx$ 500 µm was found. In another example [28] the characteristic droplet diameter d_{v50}, corresponding to 50% of the water, was measured to $d_{v50}\approx$ 900 µm in the far field from a pendent sprinkler. It must also be added that although the tests were conducted with equipment which is regularly employed by professional fire fighters, the pressure at the inlet of some of the devices seemed to be lower than specified by the manufacturer due to the equipment employed in these tests.

The size results for the cutting extinguisher shows that droplet size decreases with pressure and increases slightly with distance from the nozzle, as measured up to a distance of 15 m. The latter phenomena could possibly be explained by either coalescence or by the higher inertia of the larger droplets.

Coalescence is common in dense jets where liquid particles of equal or different sizes collide forming a new droplet. Ashgriz and Poo [29] reported different expressions to assess the coalescence region as function of the non-dimensional impact parameter x, which is a function of the relative velocity prior to the collision, the drop size ratio Δ between the colliding droplets, and Weber number of the smaller droplet. Figure 15 shows the region of coalescence and stretching separation region for droplets after an off-axis collision. The region under every curve is where coalescence is most probable while the region above the curves denote the region where stretching separation occurs.

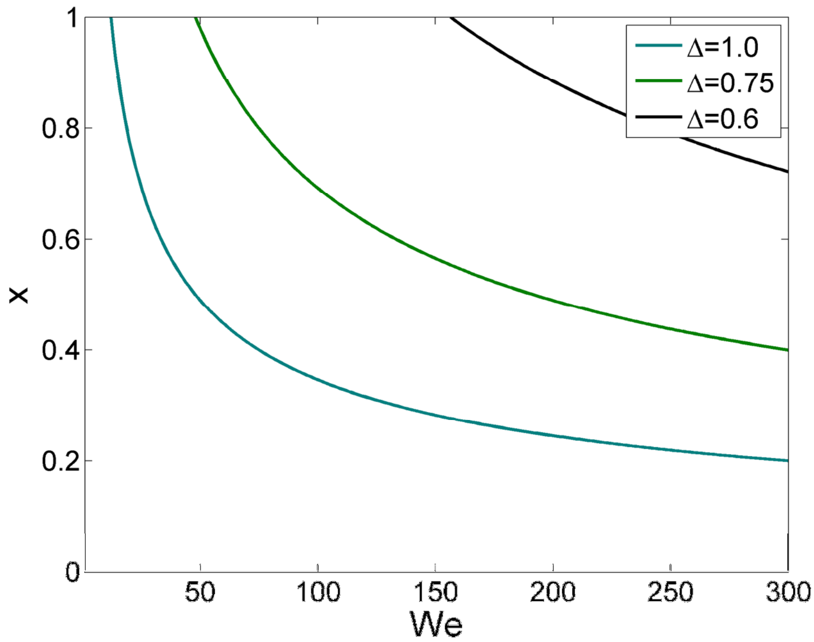

Figure 15. Coalescence and separation region for a pair of colliding droplets.

Results from the plots give an indication that coalescence can be rather probable in the spray produced by the cutting extinguisher at large distances from the nozzle, especially for a pair of droplets that are non-equal in size and having an off-axis collision (x<0.2). Droplets with diameters around 100 µm and low velocities $U < 5\ m\ s^{-1}$ have very low We numbers.

5.1 Cooling effects

As mentioned in Section 2.3.1 the droplets extract heat from flames and hot gases by heating the water from room temperature to 100°C, and by evaporation where the extracted energy is used to induce a phase change from liquid to gaseous water. The rate of transport of energy to the droplet depends on the surface area of the droplet and the relative velocity of the droplet as compared to the air [3].

The heat energy transferred to the droplet per unit time is proportional to the droplet's surface. The heating rate is proportional to the transferred power per unit volume. Therefore d_{32} is useful when comparing the heating rate of the droplets. The relative surface to volume ratio between the conventional systems and the cutting extinguisher is approximately 900/170 ≈ 5. The significance of this is that the generally smaller water droplets from the cutting extinguisher heat up much faster and extract more power from the flames and hot gases. This in turn will lead to an accelerated evaporation, resulting in enhanced inerting, see Section 5.2.

Similarly for evaporation, the available surface area per volume of water is characterized by d_{32} and the evaporation is therefore much faster with the cutting extinguisher than for the conventional systems studied.

The rate of cooling (that is heating of droplets) and evaporation discussed above is very important since if this rate is too low the droplets will hit the floor or walls before being evaporated, which reduces that overall gas-cooling efficiency [30].

The heating and evaporation also depends on the relative velocity between the droplets and the air. For small droplets this relative velocity will quickly approach zero however [3] due to the fast velocity response, see also Section 5.4.

Once evaporated the steam will be heated from 100°C to the temperature of the surrounding gases. This will further cool the gases and it is therefore important, from a gas cooling perspective, that as much water as possible is evaporated rather than being used for surface wetting. As was mentioned in Section 2.3.1 water vapor has a higher specific heat capacity than air and is therefore more efficient than air in cooling hot gases.

5.2 Inerting (reduction of the partial pressure of oxygen)

The fire can be efficiently controlled if the air is partly replaced by water vapour. This reduces the partial pressure of oxygen. This can reduce or even extinguish the fire. For example when the oxygen concentration is reduced from 21% to 13% (wood fire) or to 7% (petroleum fire) the fire will self-extinguish [3]. The evaporation rate in gas will be enhanced for fine mists according to the discussion in Section 5.1. Fast evaporation can also be achieved by pointing the spray at a hot surface. In this case it is not obvious how much the droplet size affects the evaporation rate. This will depend on the hot surface temperature, hot surface structure, etc. Clearly, when the mist is injected blind into an enclosure there is no reason to assume that the spray will hit a particularly hot surfaces. In this perspective a fine mist will unconditionally enhance the evaporation rate, and thereby also the rate at which the oxygen partial pressure is reduced.

It should be pointed out that inerting can be greatly inhibited if fresh air is entrained in the spray. Therefore, using a nozzle that can interact with the fire without the introduction of fresh air greatly enhances the extinguishing capacity of such a system, e.g. if the extinguisher can be introduced into the compartment through a minimal hole. Indeed, in such cases the system may even act to entrain vitiated air from the fire back into the combustion environment further enhancing its performance.

Effective inerting is assumed to be effective only for underventilated conditions [1]. The cooling, through heating and evaporation of the droplets, however, happens as soon as the temperature, or radiation, is high enough. It is therefore reasonable to assume that inerting could have an effect also under well ventilated conditions. More research is needed in this area to confirm this.

5.3 Reduction in radiative heat transfer

One of the major advantages with fine water mist is its ability to absorb heat radiation from a fire. This will reduce the radiative heat transfer, thereby reducing the fire spread, but it will also enhance the heating and evaporation of the droplets due to the absorbed heat radiation. In Figure 16 the volumetric absorption efficiency [31] for water droplets exposed to heat radiation corresponding to a 900°C black body radiation is shown. This property, $C'''_{abs,eff}$, is a measure of how much radiation is absorbed per unit volume of water.

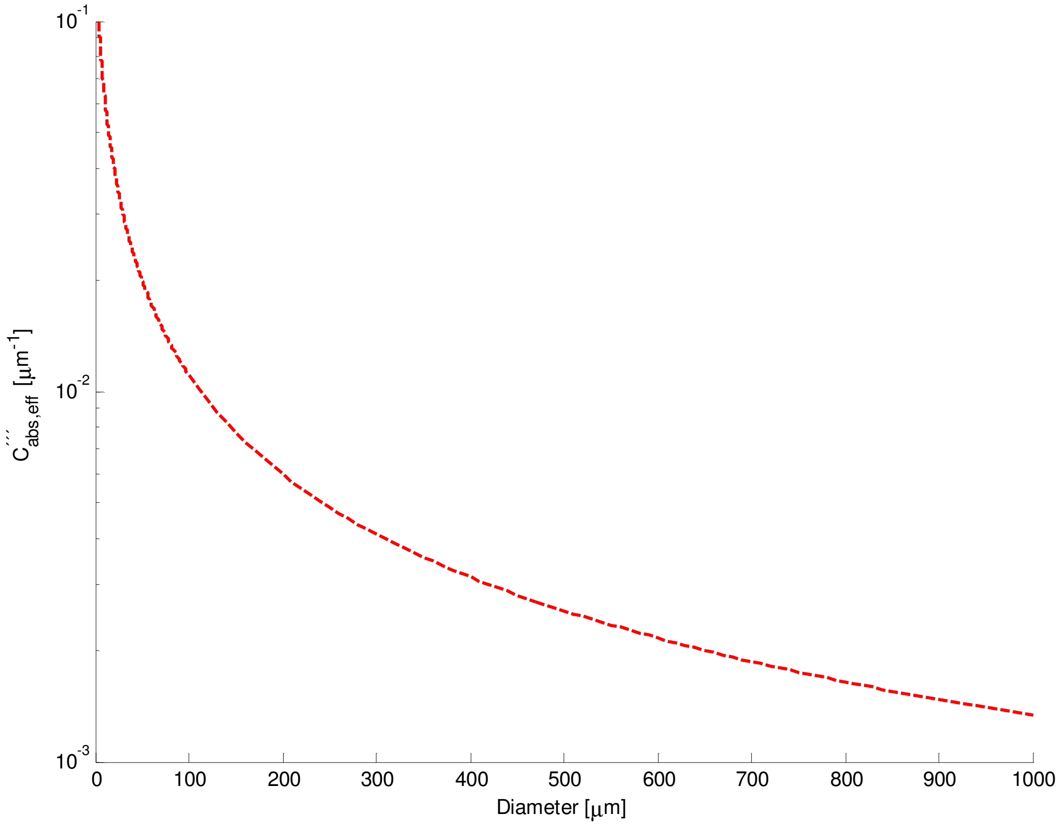

Figure 16. Volumetric absorption efficiency as a function of droplet diameter. A radiation source corresponding to 900°C black body radiation has been assumed. Adapted from [31].

As an example, comparing the d_{32} diameters 170 μm and 900 μm gives a ratio in volumetric absorption efficiency of 5. However, a rigorous evaluation should average over the product of the size histograms and the volume of the droplets.

5.4 Transport properties

Small droplets promote the fire suppressing mechanisms as discussed in Sections 5.1 to 5.3 above not only because of the mechanisms themselves (that is cooling, inerting, and radiation absorption) but also indirectly because smaller droplets will stay airborne longer than larger ones, leaving more time for these mechanisms to act on the fire.

It has been shown [2] that a droplet with 100 μm diameter entering gas phase atmosphere of 400 °C will have a lifetime of 0.2 s and will fall 30 mm before being totally vaporized. For a 1 mm droplet the corresponding values are a lifetime of 230 s and a falling distance of 680 m! Although these calculations have been performed with different diameters than those measured for the cutting extinguisher and the conventional systems in this study the comparison is still relevant. The Sauter diameter, d_{32} describes a typical diameter of the droplets and therefore the comparison between the measured d_{32}, 170 μm vs. 900 μm, is not too far from the numerical examples in reference [2]. In short this shows that when a large proportion of the water is carried in the large droplets these droplets will fall to the floor or hit a wall before being entirely evaporated. These differences in transport properties will reduce the gas cooling and inerting capacity, as well as incur larger property losses due to water damages for conventional systems as compared to high pressure water mist systems.

There are typically two contradictory requirements on the spray: rapid evaporation of droplets and strong mixing induced by the spray. Smaller droplets lead to rapid evaporation but also typically reduce the mixing. However, by using a high injection pressure the velocity and the total water amount of the spray is increased. This clearly compensates the lower mixing potential for small droplets but it is unclear by to what degree. More research is needed on this subject [3].

The particle velocity response to the fluid velocity in an accelerating flow is obtained as follows:

$$U_p(t) = U_f \left[1 - exp\left(-\frac{1}{\tau_p}\right)\right] \tag{19}$$

the particle response time τ_p is defined as follows:

$$\tau_p = \left[d_p \left(\frac{\rho}{18\mu}\right)\right] \tag{20}$$

As an example, the calculated response time for water drops of different sizes at the experimental conditions are shown:

τ_p = 3.7 µs (1 µm)
τ_p = 0.37 ms (10 µm)
τ_p = 37 ms (100 µm)
τ_p = 926 ms (500 µm)
τ_p = 3.7 s (1 mm)

It is clear that although the sedimentation time is essential, it is not the only important aspect since the ability for a particle to follow the flow of the jet is paramount for this kind of extinguishing method. It can be seen that droplets larger than 100 µm begin to show difficulty following this highly turbulent flow.

Atomization in the spray from the cutting extinguisher commences just after the liquid jet exits the nozzle and commences its interaction with the surrounding air; furthermore, the momentum of the jet induces a flow from the gas surrounding the spray into the spray itself. This can be exemplified in Figure 17 where a jet entering into the control volume induces a flow of air into the spray and transfers part of its momentum to the gas up to a point that the droplets and air leaving the control volume have almost identical velocities. This effect can promote fire suppression mechanism when vitiated air is entrained into the spray. If fresh air is entrained the fire suppression will on the contrary be inhibited, as discussed in Section 5.2. The transfer of momentum in these kinds of flows enhances the transport of droplets, transporting them much farther away than if these droplets were simply ejected into a quiescent atmosphere at high velocities.

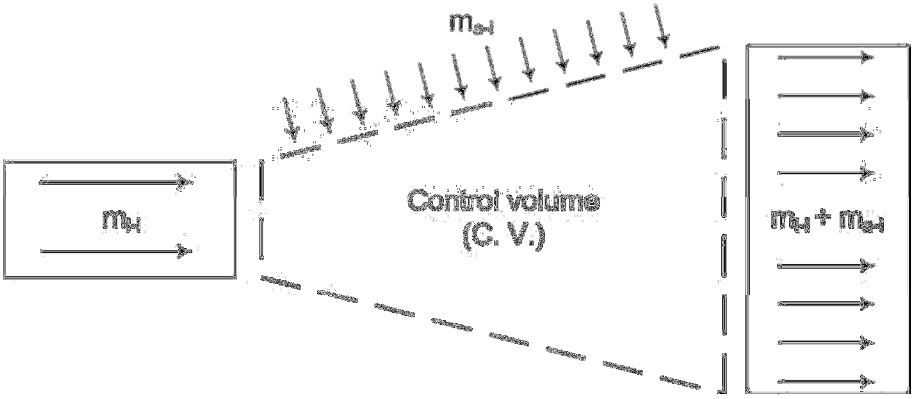

Figure 17. Control volume used for theoretical preliminary calculations.

The former discussion can be continued by contrasting the behaviour of the cutting extinguisher with the theoretical penetration of single droplets of different sizes being ejected at high velocities (U=200 ms^{-1}) into a quiescent atmosphere, as it is shown in Figure 18. These plots show that the penetration of droplets injected into air at low temperature and density is modest, even for very large drops as shown in the upper plot. On the other hand, the experiments carried out with the cutting extinguisher show that the spray produced by the cutting jet has velocities well above zero even at distances as large as fifteen metres from the nozzle. This is to a large degree a direct result of the high pressure and not an indirect result of the small droplets. The high pressure, resulting in a high speed and high flow, creates a high momentum spray that pushes the water mist long distances into an enclosure fire, making it possible to act on fires distant from the nozzle despite the small droplets.

The drag coefficient C_D for calculating the trajectories of the droplets were calculated as follows [32]:

$$C_D = \frac{24}{Re}\left(1 + \frac{1}{6}Re^{\frac{2}{3}}\right) \tag{21}$$

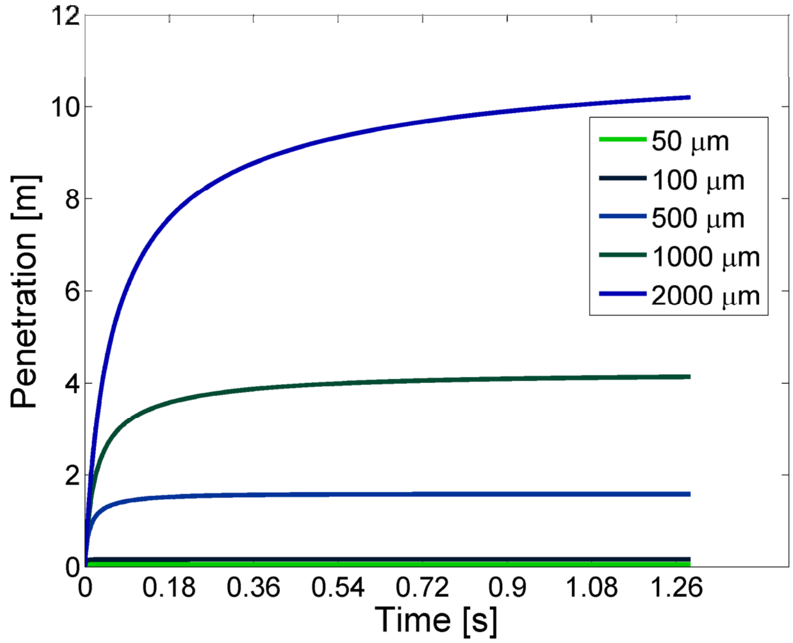

Figure 18. Theoretical penetration of single droplets into air with an initial velocity U=200 ms^{-1}.

The cone angle α/2 (see Figure 19) of the spray was determined from processing the images captured during the measuring campaign. It was found that α/2~5.7° and it is almost constant along the spray axis.

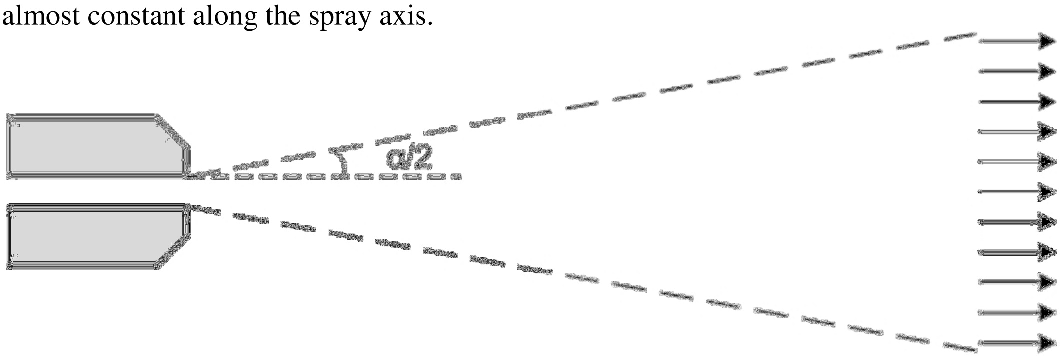

Figure 19. Sketch of the spray illustrating the cone angle.

The velocity of the spray was also theoretically estimated by assuming conservation of momentum and energy inside the control volume, given the estimated cone angle. Considering that part of the inflected energy and momentum are maintained by the flow and part used for atomization and inducing the flow from the surrounding air into the spray, the velocity of the flow at 8 m in the axial direction of the spray can be estimated around 6.3 ms^{-1}. In the GSV-measurement the spray density at 8 m was too high for reliable measurements to be performed. At 10 m the velocity was measured to 7 ms^{-1}, see Table 4, which is somewhat high as compared to theoretical calculations. In summary, the high pressure, entrained air, high spray momentum, and also the small cone angle leads to significant velocities at relatively long distances from the nozzle. This makes it possible to transport and mix the water mist much effectively that what is indicated in Figure 18. This is of importance for the extinguishing process itself but also for the feasibility of fire fighters to enter the enclosure.

6 Conclusions and outlook

Experimental measurements show that the spray from the cutting extinguisher is characterized by small droplets. The following characteristic diameters were measured at 10 m distance from the nozzle using 260 bar injection pressure: arithmetic mean diameter d_{10}≈70 µm, Sauter mean diameter d_{32}≈170 µm , and volumetric mean diameter d_{30}≈110 µm. The latter value confirms previous theoretical estimations that d_{30}≈0.1 mm. The velocity at this distance from the nozzle was approximately 7 ms^{-1} in the spray core. Droplet diameters decrease significantly when foaming agents are mixed into the water, d_{10} drops to 40 µm and d_{32} to 140 µm. Droplets also seem to be smaller outside the spray core, d_{10} drops to 40 µm and d_{32} to 100 µm at an off center distance of 80 cm from the spray axis. The volumetric capacity was 57 $lmin^{-1}$.

These measurements confirm earlier explanations of the efficiency of the cutting extinguisher, and also lead to more detailed understanding of the extinguishing effect. Cooling, inerting and radiation absorption becomes more effective with these small droplet diameters than for systems with larger droplets. Furthermore, the fact that small droplets are more prone to follow the air flow than to fall to the floor means that the time available for these suppression mechanisms to act on the fire becomes longer with smaller diameters.

The high pressure system also gives higher velocities than the other systems, i.e. 7 ms^{-1} at 10 m distance as compared to ~1 ms^{-1} at a distance of 2-4 m from the nozzle exit. The high speed and high flow creates a high momentum spray that pushes the water mist long distances into an enclosure fire, making it possible to act on fires distant from the nozzle despite the small droplets. This could also have the additional benefit in certain circumstances of entraining vitiated air into the fire by the turbulence created.

The droplet sizes for the cutting extinguisher were well characterized. For a better understanding of the transport properties information about the velocity field is needed however. The measurements presented here were of a quasi-zero-dimensional type. In order to map out flow effects, such as turbulence for example, two-dimensional information on a relatively large scale, say 1 m by 1 m, would be required. It is therefore proposed that the GSV-measurements presented in this report are complemented with PIV measurements which would give the desired information. Quantitative measurements on the inerting effects in ventilated enclosures would also be of great interest.

Comparative measurements were also performed on other firefighting systems. However, given the relatively low pressures achieved at these nozzles the sprays were not entirely of water mist type. Indeed, the measurements indicated that a significant portion of the droplet sizes were relatively large. As the alternative systems were used as comparison, no optimization of their performance was attempted in this study. A full comparison of performance capabilities in real fires would require further study.

References

[1] Bjerregaard J, Olsson D, Skärsläckaren, experimentella försök och beräkningar, Department of Fire Safety Engineering, Lund University, Lund, 2007.
[2] Gsell J, Assessment Of Fire Suppression Capabilities Of Water Mist - Fighting Compartment Fires with the Cutting Extinguisher -, Faculty of Art, Design and the Built Environment, University of Ulster, Belfast, 2010.
[3] Cutting Extinguishing Concept - practical and operational use, MSB, Swedish Civil Contingencies Agency, 2010.
[4] The Cutting Extinguisher - concept and development, Räddningsverket, Swedish Rescue Services Agency, 2001.
[5] Försth M, Sienes EdB, Andersson M, Ruuth K, Dispersion of two-phase jets from accidental releases in hydraulic pipes, SP Report 2011:23, SP Fire Technology, Borås, 2011.
[6] Lefebvre AH, Atomization and Sprays, 1 ed., Taylor & Francis, 1989.
[7] Liu H, Science and Engineering of Droplets, William Andrew Publishing, New York, 2000.
[8] Sirignano WA, Fluid dynamics and transport of droplets and sprays, Cambridge University Press, Cambridge, 1999.
[9] Korsunov YA, P. TA, Experimental investigation of liquid droplet breakup at low Reynolds numbers (in Russian). *Izv. Akad. Nauk. SSSR, Mekh Zhidk. Gaza*, 1971; **2**: 182-186.
[10] Johnson DW, Woodward JL, Release: a model with data to predict aerosol rainout in accidental releases, Wiley, New York, 1998.
[11] J. KN, Fragmentation and coalescence dynamics in multiphase flows. *Exp. Thermal Fluid Sci.*, 1993; **6**: 211-251.
[12] A. W, Deformation and breakup of liquid drops in a gas stream at nearly critical Weber numbers. *Experiments in Fluids*, 1990; **9**: 59-64.
[13] Mackrory, Characterization of black liquor sprays for application to entrained-flow processes, Brigham Young University, 2006.
[14] Hertzberg T, Hahne A, Josefsson C, Holmstedt G, Husted B, SP Rapport 2004:15 Vattendimma: Teori, fysik, simulering. Brandforsk projekt 514-021, SP Sveriges Provnings- och Forskningsinstitute, 2004.
[15] Speight J, Lange's Handbook of Chemistry (16th Edition), McGraw-Hill Professional Publishing, New York, NY, USA, 2005.
[16] Dimspik waterfog, DAFO.
[17] Handell A, Utvärdering av dimstrålrörs effektivitet vid brandgaskylning, Department of Fire Safety Engineering, Lund University, Lund, 2000.
[18] G-Force Ultiforce 150 Pulsing datasheet, Leader.
[19] Raffel M, Willert CE, Kompenhans J, Particle Image Velocimetry: A Practical Guide, Springer, 1998.
[20] Ragucci R, Cavaliere A, Massoli P, Drop sizing by laser light scattering exploiting intensity angular oscillation in the Mie regime. *Particle & Particle Systems Characterization*, 1990; **7**: 221-225.
[21] Glover AR, Skippon SM, Boyle RD, Interferometric laser imaging for droplet sizing: a method for droplet-size measurement in sparse spray systems. *Applied Optics*, 1995; **34**: 8409-8421.
[22] Pan G, Shakal J, Lai W, Calabria R, Massoli P, Simultaneous Global Size and Velocity Measurement of Droplets and Sprays: Proc. ILASS-Europe 2005, Orleans, France, 2005.
[23] Global Sizing Velocimetry, Operation Manual, TSI Incorporated, Shoreview, MN, USA, 2011.
[24] Global Sizing Velocimetry (GSV) System, TSI.
[25] White FM, Fluid Mechanics, McGraw-Hill, 2003.

[26] Särdqvist S, Vatten och andra släckmedel, Räddningsverket, 2006.
[27] Widmann JF, Characterization of a Residential Fire Sprinkler Using Phase Doppler Interferometry, National Institute of Standards and Technology, 2000.
[28] Zhou X, D'Aniello SP, Yu H-Z, Spray characterization measurements of a pendent fire sprinkler. *Fire Safety Journal*, 2012; **54**: 36-48.
[29] Ashgriz N, Poo JY, Coalescence and separation in binary collisions of liquid drops. *Journal of Fluid Mechanics*, 1990; **221**: 183-204.
[30] Larsson M, Westerlund J, Högtrycksbrandsläckning - Ett beslutsunderlag för Räddningstjänsten, Department of Fire Safety Engineering, Lund University, Lund, 2006.
[31] Försth M, Möller K, Enhanced absorption of fire induced heat radiation in liquid droplets. *submitted to Fire Safety Journal*, 2012.
[32] Ortiz C, Joseph DD, Beavers GS, Acceleration of a liquid drop suddenly exposed to a high-speed airstream. *International Journal of Multiphase Flow*, 2004; **30**: 217-234.

SP Technical Research Institute of Sweden

Our work is concentrated on innovation and the development of value-adding technology. Using Sweden's most extensive and advanced resources for technical evaluation, measurement technology, research and development, we make an important contribution to the competitiveness and sustainable development of industry. Research is carried out in close conjunction with universities and institutes of technology, to the benefit of a customer base of about 10000 organisations, ranging from start-up companies developing new technologies or new ideas to international groups.

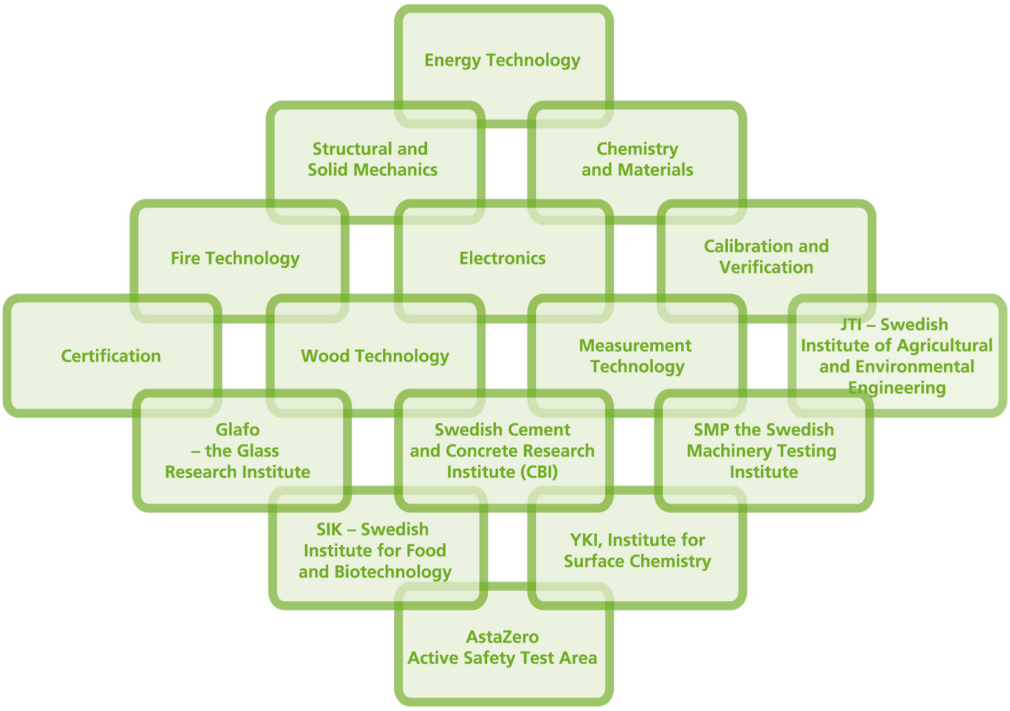

SP Technical Research Institute of Sweden

Box 857, SE-501 15 BORÅS, SWEDEN

Telephone: +46 10 516 50 00, Telefax: +46 33 13 55 02

E-mail: info@sp.se, Internet: www.sp.se

www.sp.se

Fire Technology

SP Arbetsrapport 2012:14

ISBN

ISSN 0284-5172

More information about publications published by SP: **www.sp.se/publ**